

# Farnesoid X receptor protects human and murine gastric epithelial cells against inflammation-induced damage

Fan LIAN\*, Xiangbin XING\*, Gang YUAN\*, Claus SCHÄFER†, Sandra RAUSER‡, Axel WALCH‡, Christoph RÖCKEN§, Martin EBELING||, Matthew B. WRIGHT||, Roland M. SCHMID¶, Matthias P. A. EBERT\*\* and Elke BURGERMEISTER\*\*

\*Department of Gastroenterology, The First Affiliated Hospital of Sun Yat-sen University, 510275 Guangzhou, China, †Department of Medicine II, Klinikum der Universität München, D-81377 Munich, Germany, ‡Institute of Pathology, Helmholtz Zentrum München, D-85764 Oberschleissheim, Germany, §Institute of Pathology, Christian Albrechts Universität, D-24105 Kiel, Germany, IIF. Hoffmann-La Roche, CH-4070 Basel, Switzerland, ¶Department of Medicine II, Klinikum rechts der Isar, Technische Universität München, D-81675 Munich, Germany, and \*\* Department of Medicine II, Universitätsklinikum Mannheim der Universität Heidelberg, D-68167 Mannheim, Germany

Bile acids from duodenogastric reflux promote inflammation and increase the risk for gastro-oesophageal cancers. FXR (farnesoid X receptor/NR1H4) is a transcription factor regulated by bile acids such as CDCA (chenodeoxycholic acid). FXR protects the liver and the intestinal tract against bile acid overload; however, a functional role for FXR in the stomach has not been described. We detected FXR expression in the normal human stomach and in GC (gastric cancer). FXR mRNA and protein were also present in the human GC cell lines MKN45 and SNU5, but not in the AGS cell line. Transfection of FXR into AGS cells protected against TNF $\alpha$  (tumour necrosis factor  $\alpha$ )-induced cell damage. We identified K13 (keratin 13), an anti-apoptotic protein of desmosomes, as a novel CDCA-regulated FXR-target gene. FXR

bound to a conserved regulatory element in the proximal human K13 promoter. Gastric expression of *K13* mRNA was increased in an FXR-dependent manner by a chow diet enriched with 1 % (w/w) CDCA and by indomethacin (35 mg/kg of body weight intraperitoneal) in C57BL/6 mice. FXR-deficient mice were more susceptible to indomethacin-induced gastric ulceration than their WT (wild-type) littermates. These results suggest that FXR increases the resistance of human and murine gastric epithelial cells to inflammation-mediated damage and may thus participate in the development of GC.

Key words: bile acid, chenodeoxycholic acid (CDCA), farnesoid X receptor (FXR), keratin, gastric cancer, stomach.

# INTRODUCTION

Overexposure to bile acids leads to damage of GI (gastrointestinal) epithelia. For example, patients with recurrent heartburn are at increased risk of oesophageal cancer [1]. Chronic inflammation upon duodenogastric reflux of bile acids, e.g. after gastric resection, is an important risk factor for GC (gastric cancer) [2–5]. Efficient detoxification mechanisms, some involving members of the nuclear receptor superfamily [6], counteract the detrimental actions of excess bile acids on GI organs.

FXR (farnesoid X receptor/NR1H4) is nuclear receptor and transcription factor activated by physiological bile acids [6,7] including CDCA (chenodeoxycholic acid) and DCA (deoxycholic acid). FXR suppresses the *de novo* synthesis of bile acids in the liver and promotes excretion and enterohepatic circulation of conjugated bile acids [8]. Previous studies in FXR-deficient mice have suggested a beneficial role for FXR against cholestasis [7] and colitis [9]. FXR facilitates liver regeneration, supports the differentiation of the intestinal epithelium and promotes antibacterial defence in the GI tract [7]. In contrast, FXR-deficiency exacerbates hepatic [7] and intestinal [9] inflammation and promotes carcinogenesis in mice [10]. These results corroborate the idea that FXR acts as a protective factor in the liver and the GI tract.

Aberrant FXR expression or function has also been detected in human adenocarcinomas of the colon [11], breast [12], prostate

[13] and oesophagus [Barrett's IM (intestinal metaplasia)] [14]. These findings pointed to either causative or protective roles for bile acids and/or FXR in the pathogenesis of these tumour types. FXR mRNA variants have been identified in normal stomach tissue of humans and mice [15,16]; however, a functional role for gastric FXR has not yet been defined. We therefore have evaluated the role of bile-acid-activated FXR on cell survival of human and mouse gastric epithelial cells. The results of the present study indicate that FXR increases the resistance to inflammation-induced cell damage accompanied by the upregulation of protective target genes, such as K13 (keratin 13).

## MATERIALS AND METHODS

# **Subjects**

Tumour specimens were obtained by surgical resection from GC patients and processed according to standard methods [17]. TMAs (tissue microarrays) were then generated. GC was classified histologically into D-T (diffuse-type), I-T (intestinal-type) and undifferentiated types according to the Lauren classification [17a]. IM-T (IM-type) was assessed within I-T tissue specimens. Tissue sample collection of human GC specimens was approved by the Ethics Committees of the Technische Universität München and the Charité Berlin. Written informed consent was received from the patients used in this study.

Abbreviations used: BSEP, bile salt export pump; CDCA, chenodeoxycholic acid; ChIP, chromatin immunoprecipitation; CHX, cycloheximide; D-T, diffuse-type; EMSA, electrophoretic mobility-shift assay; EV, empty vector; FXR, farnesoid X receptor; GC, gastric cancer; GI, gastrointestinal; HCC, hepatocellular carcinoma; H&E, haematoxylin and eosin; HEK, human embryonic kidney; IBABP, ileal bile-acid-binding protein; IHC, immunohistochemistry; IL, interleukin; IM, intestinal metaplasia; IM-T, IM-type; Indo, indomethacin; IR1, inverted repeat 1; I-T, intestinal-type; K13 etc., keratin 13 etc.; KO, knockout; MTT, 3-(4,5-dimethylthiazol-2-yl)-2,5-diphenyl-2H-tetrazolium bromide; OST $\alpha$ , organic solute transporter  $\alpha$ ; PARP, poly(ADP-ribose) polymerase; PI, propidium iodide; qPCR, quantitative PCR; RARE, retinoic acid receptor-responsive element; RNAi, RNA interference; RT, reverse transcription; SHP, small heterodimer partner; siRNA, short interfering RNA; TMA, tissue microarray; TNF, tumour necrosis factor; WB, Western blotting; WT, wild-type.

To whom correspondence should be addressed (elke.burgermeister@lrz.tum.de).

#### **Animal studies**

WT (wild-type) and FXR (Nr1h4/UniProtKB/Swiss-Prot number Q60641)-KO (knockout) mice (strainB6; 129XFVB-Nr1h4-tm1Gonz/J, Jackson Laboratory) were maintained on a pure C57BL/6 background. Male mice (4-weeks-old) received a chow diet (Altromin) containing 1 % (w/w) CDCA (Chemos) (n = 5 per group and genotype). Experimental gastric ulceration ( $n \ge 6$  per group and genotype) was performed with Indo (indomethacin) as described previously [18]. Animal housing and experiments were performed in agreement with the ethical guidelines of the Technische Universität München and the Ludwig Maximillians Universität München, and were approved by the appropriate government authorities.

# Cell culture and WB (Western blotting)

HEK (human embryonic kidney)-293, hepatoma HepG2 and the GC cell lines AGS, NCI-N87, SNU1, SNU5, KATOIII (A.T.C.C.), MKN7 and MKN45 (Japan Cell Bank) were cultivated as described previously [17]. Stable AGS clones were generated [17] upon transfection with full-length human FXRα1 cDNA (GenBank® accession number NM\_001206977.1) in pTarget (AGS/FXR) or pTarget EV (empty vector) (AGS/EV) respectively. SDS/PAGE (12 % gel) and WB of cell and tissue lysates (25  $\mu$ g of protein per gel lane) were performed as described previously [17].

#### **Antibodies**

The anti-FXR (H-130; Santa Cruz Biotechnology) and anti-K13 (NCL-K13; Novocastra) antibodies were used for IHC (immunohistochemistry) and WB. Anti-FXR (clone A9033A; R&D Systems), anti-(cleaved caspase 8) (Asp<sup>391</sup>) (18C8) and anti-(cleaved caspase 3) (Asp<sup>175</sup>) (Cell Signaling Technology), anti-(cleaved PARP) [poly(ADP-ribose) polymerase] (Asp<sup>214</sup>) (7C9; Cell Signaling Technology) and anti- $\beta$ -actin (clone AC-74; Sigma) were used for WB.

# IHC

Sections from paraffin-embedded tissues (3  $\mu$ m) were stained (1:100, FXR H-130) as described previously [19]. Cryosections (10  $\mu$ m) were stained (1:50, K13) following antigen retrieval using pepsin digestion and the Vectastain® Mouse-on-Mouse kit (Vectorlabs). The TMAs were subjected to an automated staining protocol and quantitatively evaluated by an expert pathologist.

#### **DNA** constructs

The FXR-RE (responsive element) reporter plasmid consists of the human BSEP (bile salt export pump) promoter driving the luciferase gene in pTK-luc (FXR-RE-luc) [20]. The human K13 promoter (GenBank® accession number AF049259, 1-525 bp) containing a putative FXR site (RARE2) was subcloned into pGL3-basic-luc (Promega) (RARE2-WT-K13pluc) [21]. A second plasmid (RARE2-MUT-K13p-luc) was constructed, in which the ACTGGGTGGGGCTCA (RARE2) element in the human K13 promoter was deleted using the QuikChange® kit (Stratagene). The 1428 bp full-length human FXR cDNA (476 amino acids, α1 splice variant with additional four amino acids MYTG; GenBank® accession number NM\_001206977.1) [16] was inserted into pTarget (Promega). SiGENOME SMARTpool siRNA (short interfering RNA) against human FXR and K13 was from Dharmacon. Knockdown efficiency was verified by RT (reverse transcription)-

qPCR (quantitative PCR) and WB, and varied between 40 to 80%. PCR products for human FXR $\alpha$ 1/2 (GenBank® accession numbers NM\_001206977.1 and NM\_001206978.1) and FXR $\alpha$ 3/4 (GenBank® accession numbers NM\_01206993.1 and NM\_001206992.1) mRNA variants [22] (Supplementary Table S1 at http://www.BiochemJ.org/bj/438/bj4380315add.htm) were purified from agarose gels (Invitrogen) and confirmed by sequencing (GATC).

# RT-PCR and qPCR

Reactions were performed as described previously [19].  $C_T$ -values were normalized to  $C_T$  values of  $\beta_2$ -microglobulin and compared with 'no template' controls (CT>36).

## **DNA** microarrays

AGS/FXR and AGS/EV cells were treated for 16 h with  $100 \,\mu\text{M}$  CDCA. cRNAs were produced as described by the manufacturer (One-Cycle cRNA labelling kit; Affymetrix) and hybridized to GeneChip® Human Genome Arrays (HG U133 Plus 2.0; Affymetrix) [20]. Gene sets (Supplementary Table S2 at http://www.BiochemJ.org/bj/438/bj4380315add.htm) were identified using the DAVID Bioinformatics resource (http://david.abcc.ncifcrf.gov).

# ChIP (chromatin immunoprecipitation) and EMSA (electrophoretic mobility-shift assay)

ChIP and EMSA were performed using oligonucleotides (Supplementary Table S1) as described previously [20].

# Cell viability assays

Colorimetric MTT [3-(4,5-dimethylthiazol-2-yl)-2,5-diphenyl-2H-tetrazolium bromide] assays were performed according to the manufacturer's instructions (Roche Diagnostics). Flow cytometry was done on cells grown to confluency in six-well plates and treated with TNF $\alpha$  (tumour necrosis factor  $\alpha$ ; 100 ng/ml) (Roche) and CHX (cycloheximide; 20  $\mu$ g/ml) for 6 h. Floating and adherent cells were harvested into PBS and collected by centrifugation [200 g for 4 min at room temperature (20 °C)]. Annexin and PI (propidium iodide) double staining was performed according to the manufacturer's protocols (Roche) and was analysed on a FACScalibur device (BD Biosciences).

# **Statistics**

Results are expressed as means  $\pm$  S.E.M. from at least five animals per group and genotype or three independent cell experiments. *P* values were calculated using Graphpad Prism 4 software with one-way ANOVA for mice, Student's *t* test for cells and Wilcoxon signed-rank test for patient data.

# **RESULTS**

# Expression of FXR in human GC tissues and cell lines

To assess the expression of FXR protein (NR1H4/UniProtKB/Swiss-Prot number Q96RI1) in human GC, IHC on tissue microarrays was performed using a rabbit polyclonal FXR antiserum [13,23,24] (Figure 1A). In tissues from healthy individuals, FXR was found in the nuclei of cells of the non-neoplastic foveolar epithelium from gastric glands. In a series of GC specimens (n = 70), consisting of both I-T and D-T GC, FXR was undetectable (score 0 on the Lauren classification) in

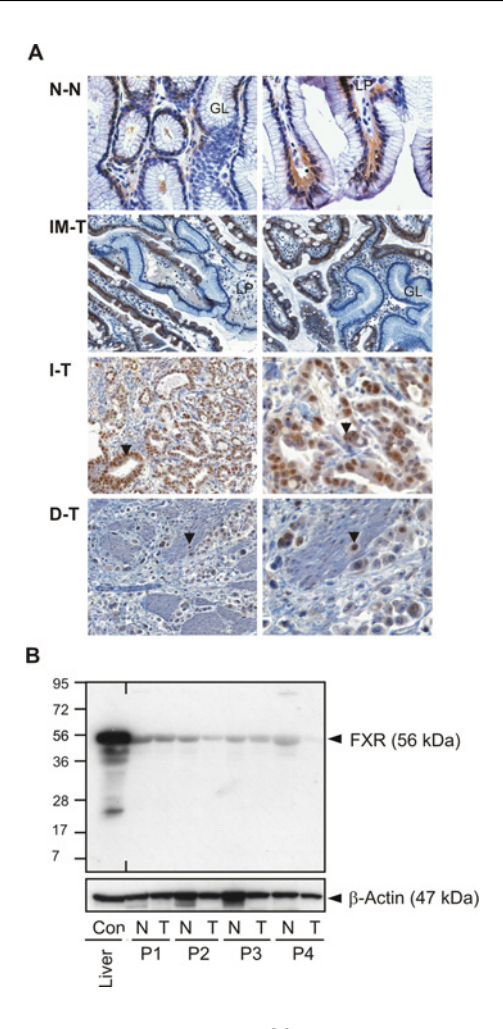


Figure 1 Expression of FXR in human GC tissue

(A) Detection of FXR (NR1H4/UniProtKB/Swiss-Prot number Q96RI1) on human GC TMAs (n=70) by IHC using the rabbit polyclonal antibody. Magnifications  $100\times$  and  $200\times$ . N-N, normal non-neoplastic gastric epithelium with nuclear FXR (score 1+); IM-T, IM in GC with strong nuclear and cytoplasmic FXR (score 2+); I-T, I-T GC positive for nuclear FXR (arrow, score 2+); D-T, D-T GC with nuclear FXR (arrow, score 1+); LP, lamina propria; GL, gland. (B) Detection of the  $\sim$ 56 kDa FXR protein in whole-tissue lysates (1+) g of protein per lane) of GC specimens by WB using the mouse monoclonal antibody; T, tumour; N, matched non-tumour sample; P, patient; Con, normal liver.

32 cases (46%), showed moderate expression (score 1+) in 31 cases (44%) and strong expression (score 2+) in seven cases (10%) in the tumour cells. FXR was most prominently expressed (score 2+) in six out of the seven specimens of I-T GC which contained regions of IM, as evident by translucent goblet cells, and was localized both in the nucleus and the cytoplasm. FXR was detected by WB in gastric tissue lysates as a  $\sim$ 56 kDa band similar in size to that detected in normal human liver using a mouse monoclonal antibody [14,25] (Figure 1B). Collectively, these data indicated that FXR is expressed in the normal human stomach and in GC.

In humans [16] and rodents [15], two major FXR mRNA variants  $\alpha 1/2$  and  $\alpha 3/4$  have been identified that result in divergence in the N-terminal region of the protein (Figure 2A) [22]. In addition, the  $\alpha 1$  and  $\alpha 3$  variants contain a four-aminoacid (MYTG) insertion of unknown function [22]. We amplified the human full-length FXR $\alpha 1/2$  mRNA with a forward primer specific for exon 1 and the truncated  $\Delta$ FXR $\alpha 1/2$  transcript with a primer specific for exon 3 that contains the start codon (GenBank® accession numbers NM\_001206977.1 and NM\_001206978.1).

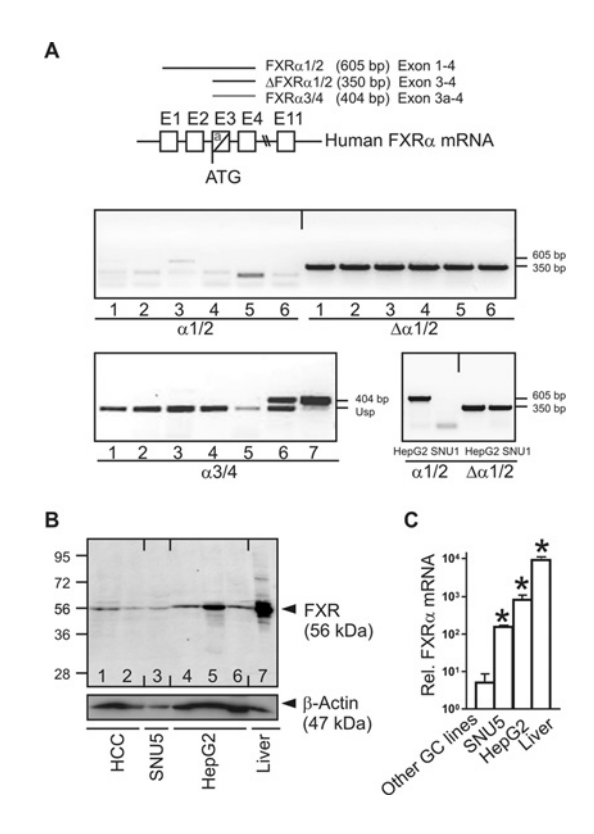


Figure 2 Expression of FXR in human GC cell lines

(A) Detection of FXR $\alpha$  mRNA splice variants ( $\alpha$ 1/2, GenBank® accession numbers NM\_001206977.1/NM\_001206978.1;  $\alpha$ 3/4, GenBank® accession numbers NM\_001206993.1/NM\_001206992.1) in human GC cell lines by RT—PCR and ethidium bromide gel electrophoresis. Lane numbers (middle panel): 1, AGS; 2, MKN45; 3, KATOIII; 4, SNU1; 5, SNU5; and 6, N87. Lane numbers (bottom panel): 1, AGS; 2, SNU1; 3, N87; 4, KATOIII; 5, MKN7; 6, MKN45; and 7, SNU5. Human hepatoma cells HepG2 were used as a positive control (lower right-hand panel). (B) Detection of the  $\sim$ 56 kDa human FXR protein in whole-cell and-tissue lysates (25  $\mu$ g of protein per lane) by WB using the mouse monoclonal antibody. Lane numbers: 1 and 2, HCC from two individual patients; 3, SNU5; 4 – 6, human HepG2 hepatoma cells from three independent culture passages; 7, normal human liver tissue. Molecular mass is given in kDa on the left-hand side. (C) Quantification of total FXR $\alpha$  mRNA (GenBank® accession number NM\_0012069) in SNU5 cells compared with other human GC cell lines (AGS, SNU1, N87, KATOIII, MKN7 and MKN45), HepG2 cells and human liver tissue. Normalized C<sub>T</sub> values from RT—qPCRs are given as the fold change  $\pm$  S.E.M. (n = 3); \*P < 0.05.

Human FXRα3/4 mRNA was detected by an exon 3a-specific primer (GenBank® accession numbers NM 001206993.1 and NM 001206992.1) [16]. A common reverse primer against exon 4 was applied for all RT-PCRs, and all PCR products were confirmed by DNA sequencing. We detected full-length FXR $\alpha$ 1/2 mRNA in human hepatoma HepG2 cells. FXRα3/4 mRNA was detected in the human GC cell lines MKN45 and SNU5. None of the other human GC cell lines (AGS, SNU1, N87, KATOIII and MKN7) expressed either full-length FXR $\alpha$ 1/2 mRNA or  $\alpha$ 3/4 mRNA; however, the  $\Delta$ FXR $\alpha$ 1/2 mRNA was detectable in all GC lines. Consistent with the results obtained from the PCR analyses, a ~56 kDa FXR protein was observed in SNU5 (Figure 2B, lane 3) cells as compared with protein lysates from human hepatoma HepG2 cells, HCC (hepatocellular carcinoma) and normal liver tissue (Figure 2B). No FXR protein was detectable in AGS, SNU1, N87, MKN7 or KATOIII cell lysates (results not shown), indicating that the  $\Delta FXR\alpha 1/2$  transcript is not translated into a detectable protein. Real-time RT-qPCR using primers against the common DNA-binding domain of FXR (GenBank® accession number NM\_0012069) confirmed that SNU5 expressed the highest levels of total FXR $\alpha$  mRNA of all the tested human GC cell lines (Figure 2C).

# FXR protects against cell damage

To explore the function of gastric FXR in cells, AGS cells were stably transfected with an expression plasmid harbouring the full-length human FXRα1 cDNA (AGS/FXR; GenBank® accession number NM\_001206977.1) or with EV (AGS/EV). Chronic inflammation is a risk factor associated with human GC [26]. The present study tested whether FXR modulates the sensitivity of AGS cells towards inflammation-induced stress in the presence of TNF $\alpha$  and CHX, which specifically induce apoptotic cell death [27]. AGS/FXR and AGS/EV cells were treated for 24 h with a mixture of TNF $\alpha$  (100 ng/ml) and CHX (20  $\mu$ g/ml). The results from MTT assays demonstrated that AGS/FXR cells retained higher viability (3-fold, P < 0.05) than AGS/EV cells (Figure 3A). CDCA (at 50  $\mu$ M) increased further the protective effect of FXR (4-fold, P < 0.05) compared with both the vehicle and CDCA-treated AGS/EV cells. SNU5 cells, which expressed the highest level of endogenous FXR, were the most resistant to the apoptotic effect of TNF $\alpha$  and CHX of all parental GC lines and comparable with HepG2 cells (results not shown), suggesting endogenous FXR is also protective.

Increased apoptosis was confirmed by WB that showed cleaved caspase 8 appearing after 6–8 h of TNF $\alpha$  and CHX treatment, followed by appearance of cleaved caspase 3 and PARP after 10 h (Figure 3B). The abundance of the cleavage products was decreased and the time of their appearance was delayed in AGS/FXR compared with AGS/EV cells. These results suggest that FXR delays and limits the activation of TNF $\alpha$ -triggered apoptosis. To quantitatively assess apoptotic cell numbers, annexin/PI dye-exclusion flow cytometry was performed. Statistical analysis of the FACS results revealed that approximately 5-fold more annexin-positive apoptotic cells were present following 6 h of treatment with TNF $\alpha$  and CHX in AGS/EV (25  $\pm$  5%, P < 0.05) than in AGS/FXR (5  $\pm$  10%) cells (Figure 3C). These results corroborate the protective effect of FXR against inflammation-mediated cell death.

# Human K13 is a novel FXR-target gene

To identify potential mechanisms underlying cell protection by FXR, AGS/FXR and AGS/EV clones were treated with 100 μM CDCA for 16 h, and total RNAs were subjected to DNA microarray analysis (see Supplementary Table S5 at http://www.BiochemJ.org/bj/438/bj4380315add.htm). Comparative analysis identified K13 mRNA (GenBank® accession number NM\_002274.3, variant b) as the most highly up-regulated transcript in AGS/FXR compared with AGS/EV cells. Other keratin types, including K6, keratin-associated protein 2-1 and plakophilin 4, a structural component of desmosomes, were also increased (Supplementary Table S2). The mRNAs for TNFAIP8 (TNF $\alpha$ -induced protein 8), an inhibitor of caspases and antiapoptotic factor, and the gastroprotective protein SERPINB2 (plasminogen activator inhibitor 2) were also specifically increased in AGS/FXR cells [28]. Induction of the human organic solute transporter  $OST\alpha$ , a well-characterized FXR-target gene, confirmed that FXR activity was increased by CDCA in AGS/FXR cells.

RT–qPCR expression analysis was performed to confirm the microarray results. Treatment for 24 h with 75  $\mu$ M CDCA up-regulated K13 mRNA (4-fold) and the FXR-target genes OST $\alpha$  (2-fold) and IBABP (ileal bile-acid-binding protein) (36-fold) in AGS/FXR cells (P < 0.05), but not in AGS/EV cells (Figure 4A). Using WB it was demonstrated that the  $\sim$ 54 kDa K13 protein (K1C13/UniProtKB/Swiss-Prot number P13646) was also increased in parallel with its mRNA (Figure 4B).

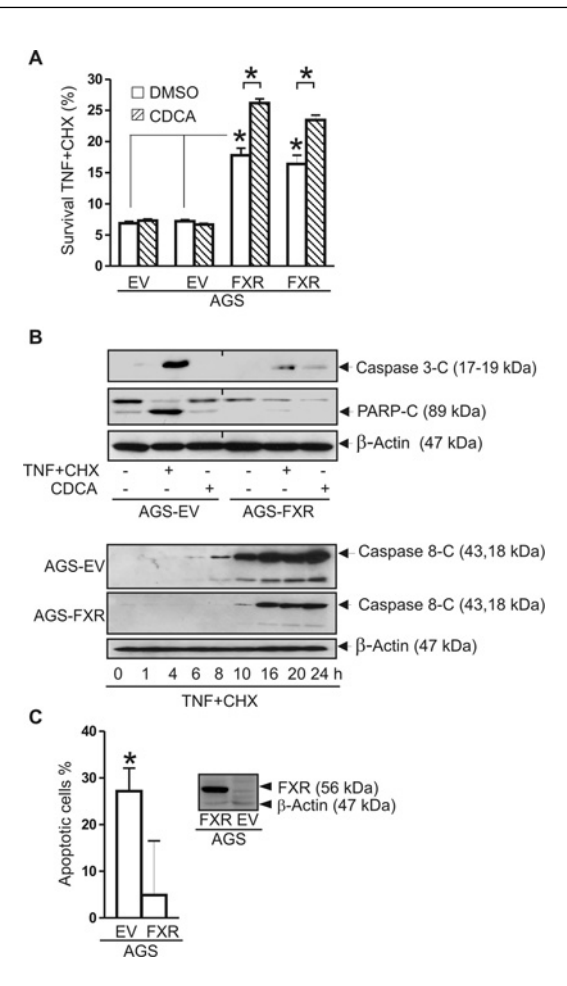


Figure 3 FXR protects against apoptotic cell death

(A) AGS clones were stably transfected with FXR $\alpha$ 1 cDNA (AGS/FXR, GenBank® accession number NM\_001206977.1) or EV (AGS/EV), respectively, and treated for 24 h with TNF $\alpha$  and CHX (100 ng/ml and 20  $\mu$ g/ml) in the presence of DMS0 or CDCA (50  $\mu$ M). Absorbance values from MTT assays are presented as the percentage  $\pm$  S.E.M. survival (n=4) of controls without TNF $\alpha$  and CHX. \*P<0.05. (B) Detection of cleaved caspase 8, caspase 3 and PARP by WB. AGS clones were treated for 6 h (upper panel) or for the times indicated (lower panel) with TNF $\alpha$  and CHX as in (A). (C) Flow cytometric (FACS) analysis of apoptosis. AGS clones were treated for 6 h as in (B). Annexin-positive and PI-negative apoptotic cells were counted and are expressed as the percentage  $\pm$  S.E.M. of the total cells (n=4). \*P<0.05. Insert: WB validating FXR overexpression in AGS clones.

CDCA also increased K13 and OST $\alpha$  mRNA (~2-fold, P < 0.05) in the parental SNU5 and MKN45 cells (results not shown), indicating that K13 is also regulated by endogenous FXR. To further test their role in apoptosis protection, both FXR and K13 expression were knocked-down by transient transfection of siRNA oligonucleotides into AGS/FXR cells, followed by a 24 h challenge with TNF $\alpha$  and CHX (100 ng/ml and 20  $\mu$ g/ml respectively) in absence and presence of 50  $\mu$ M CDCA (Figure 4C). The survival rate of RNAi (RNA interference)-treated cells was lower (~25–60%, P < 0.05) than for mock-transfected cells, both in vehicle- and CDCA-treated cultures. Similar results were obtained after FXR silencing in MKN45 and HepG2 cells (results not shown), suggesting an anti-apoptotic role also for endogenous FXR.

# FXR directly binds to and transactivates the human K13 gene promoter

In the human K13 proximal promoter (GenBank® accession number AF049259) binding sites for retinoic acid [21] and

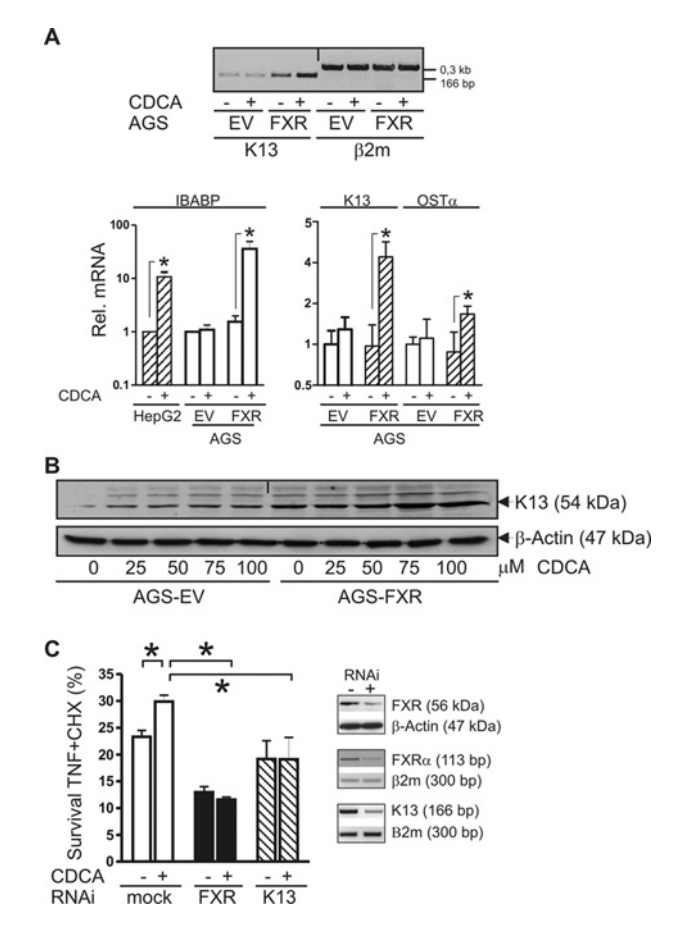


Figure 4 Human K13 is a novel FXR-target gene in vitro

(A) CDCA induces mRNA of K13 (GenBank® accession number NM\_002274.3) and FXR-target genes. AGS clones were treated with 50  $\mu$ M CDCA for 24 h. Representative ethicium bromide agarose gels of RT–PCRs are shown above the quantitative analyses. Normalized  $C_T$  values of RT–qPCRs were calculated as the fold change  $\pm$  S.E.M. (n=3) of vehicle-treated EV cells. \*P < 0.05. (B) CDCA up-regulates K13 (K1C13/UniProtKB/Swiss-Prot number P13646) protein. Representative immunoblots are shown. (C) siRNA knock-down of FXR or K13 reduces cell survival. AGS/FXR cells were mock-transfected or transfected with siRNA for 24 h and then treated as in (A). The MTT assays are presented as the percentage  $\pm$  S.E.M. survival of controls without TNF $\alpha$  and CHX. \*P < 0.05. Insert: knock-down efficiency of FXR/K13 mRNA and/or protein by siRNAs compared with  $\beta$ -actin (WB) or  $\beta_2$ -microglobulin (RT–PCR).

vitamin D<sub>3</sub> receptors have been predicted (M. Ebeling, unpublished work), and its regulation by retinoids has been shown experimentally in vitro [29,30] and in vivo [31,32]. To determine whether FXR binds to these elements, we designed ChIP primers flanking the first 500 bp upstream to the predicted transcriptional start site (Figure 5A). AGS/EV and AGS/FXR cells were incubated for 16 h with either vehicle or 75  $\mu$ M CDCA, and cell lysates were subjected to ChIP. Genomic qPCRs were visualized by gel electrophoresis and quantified (Figure 5B). No pull-down of genomic DNA was observed with agarose beads coupled to control IgG (Figure 5B, lane 3). ChIP against FXR revealed an increased FXR binding (2-fold, P < 0.05) to the K13 promoter amplicon in the presence of CDCA (Figure 5B, lane 2) compared with the vehicle (Figure 5B, lane 1) in AGS/FXR cells, but not in AGS/EV cells. These results indicate that CDCA increases FXR binding within the proximal K13 promoter.

To determine whether this genomic region mediates CDCA-and FXR-dependent transactivation of a heterologous gene [20], we cloned the proximal human K13 (-500/+1) promoter (GenBank® accession number AF049259) into pGL3-basic

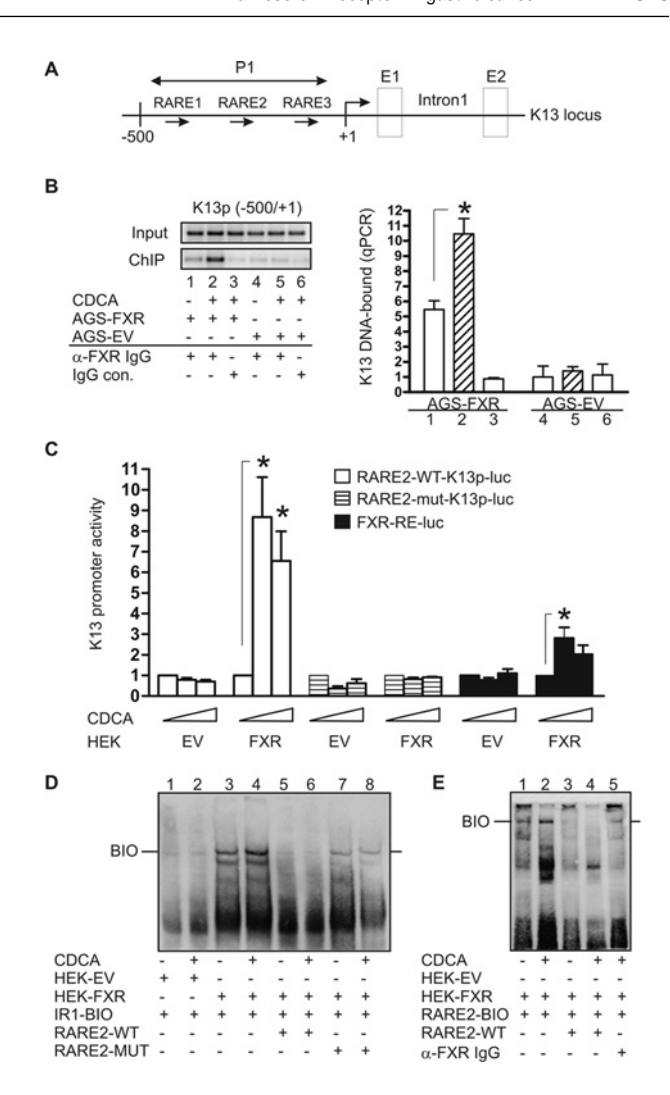


Figure 5 The human K13 promoter is bound and transactivated by FXR

(A) Scheme of the human K13 gene locus (GenBank® accession number AF049259) with predicted binding sites for RAREs. (B) AGS/EV and AGS/FXR clones were treated for 24 h with vehicle or CDCA (50  $\mu$ M). Cell lysates were subjected to immunoprecipitation with the rabbit polyclonal FXR antibody or control IgG as indicated (lanes 1-6). C<sub>T</sub> values of immunoprecipitated DNA normalized to  $C_T$  values of input DNA are expressed as the fold change  $\pm$  S.E.M. (n = 2) of pull-down compared with control IgG. Agarose gels (left-hand panel) and quantitative summary of genomic PCRs (right-hand panel) are presented together, \*P < 0.05. (C) HEK-293 cells were transiently co-transfected with reporter plasmids containing the human proximal K13 promoter (RARE2-WT-K13p-luc), a mutated K13 promoter (RARE2-MUT-K13p-luc) or a positive control plasmid containing a cognate FXR-responsive element from the BSEP promoter (FXR-RE-luc) together with FXR or EV expression plasmids. Cells were then treated for 24 h with CDCA (0, 30 or 100  $\mu$ M). Luciferase counts were normalized to protein content and are presented as fold change  $\pm$  S.E.M. (n=3) compared with the vehicle. \*P<0.05, CDCA compared with DMSO. (D and E) EMSA. HEK-293 cells were transfected with FXR or EV expression plasmids and stimulated with CDCA (100  $\mu$ M) for 16 h. Nuclear extracts were incubated with biotin-labelled (D) IR1 consensus FXR-binding element (IR1-BIO) [20] or (E) K13 promoter oligonucleotide (RARE2-BIO). Reaction mixtures were co-incubated with the rabbit polyclonal FXR antibody directed against the DNA-binding domain (E, lane 5) or unlabelled competitor oligonucleotides (RARE2-WT, RARE2-MUT) respectively.

luciferase vector (Figure 5C). HEK-293 cells [20] were transiently transfected with either EV or FXR expression plasmids, together with the reporter plasmid driven under the control of the K13 promoter (RARE2-WT-K13p-luc) or a control reporter plasmid containing a cognate FXR-RE from the BSEP promoter (FXR-RE-luc). The cells were treated for 24 h with 30 and 100  $\mu$ M CDCA and luciferase activity was determined in cell lysates. CDCA strongly stimulated the activity of the K13 promoter

(7–9-fold, P < 0.05) only in cells co-transfected with the FXR expression plasmid (Figure 5C).

Despite these findings, a classical IR1 (inverted repeat 1) element was not identified in the proximal 500 bp of the K13 promoter (GenBank® accession number AF049259). Nevertheless, FXR also recognizes hexameric direct repeat elements with a variable number of intervening nucleotides between the half sites [33]. Within the region amplified in our ChIP experiments, we localized three half site AGGTCAlike elements that had previously been described as RAREs (retinoic acid receptor-responsive elements) [21]. One of these half sites (RARE2) was well-conserved between human and rodents and overlapped with an experimentally proven RARE [34] and a predicted SP1 [21] site (Supplementary Table S3 at http://www.BiochemJ.org/bj/438/bj4380315add.htm). The RARE2 element was specifically deleted in the K13 promoterluciferase expression construct (RARE2-MUT-K13p-luc), and we repeated the reporter gene assay in HEK-293 cells. Deletion of RARE2 abrogated the CDCA- and FXR-dependent transcriptional activation of the K13 promoter (Figure 5C), demonstrating that RARE2 is necessary for the transcriptional activity of FXR.

To explore the direct interaction of FXR with the K13 promoter, EMSAs were performed [20] using a biotin-labelled oligonucleotide, which contained a consensus IR1 element. Nuclear extracts were prepared from HEK-293 cells that had been transiently co-transfected with FXR or EV plasmids. Increased protein binding to the IR1 element was visible in the nuclear extracts from CDCA-treated FXR-transfected cells compared with untransfected cells (Figure 5D, lanes 2 and 4 respectively). Both the basal and CDCA-dependent (Figure 5D, lanes 3 and 4 respectively) complexes were effectively reduced by competition with an unlabelled RARE2 oligonucleotide (Figure 5D, lanes 5 and 6), but not by a mutated RARE2 sequence (Figure 5D, lanes 7 and 8). Direct binding of FXR to a biotin-labelled RARE2 oligonucleotide was then tested (Figure 5E). Nuclear extracts of FXR-transfected and CDCA-treated cells produced an enhanced mobility shift compared with vehicle-treated samples (Figure 5E, lanes 2 and 1 respectively), which was efficiently competed by an excess of unlabelled RARE2 oligonucleotide (Figure 5E, lanes 3 and 4), but not by the mutated RARE2 oligonucleotide (results not shown). Addition of polyclonal FXR antiserum (1  $\mu$ g), which recognizes the DNA-binding domain of FXR, interfered with the band shift (Figure 5E, lane 5), corroborating that the DNA–protein complex observed (Figure 5E, lane 2) contains FXR bound to the RARE2 element. These results indicate that FXR binds RARE2 driving the bile-acid responsiveness of the K13 promoter.

## K13 is also regulated by FXR in vivo

To examine K13 regulation by FXR *in vivo*, WT and FXR-KO mice were fed on a chow diet enriched in 1% (w/w) CDCA for 7 days (n=5 per group and genotype). This diet was well tolerated and elicited a general FXR response in the GI tract [20]. Nuclear FXR (Nr1h4/UniProtKB/Swiss-Prot number Q60641) was visualized by IHC in the corpus and antral glands of the mouse stomach using the rabbit polyclonal antibody (Supplementary Figure S1 at http://www.BiochemJ.org/bj/438/bj4380315add.htm). Murine K13 protein (K1c13/UniProtKB/Swiss-Prot number P08730) was mainly expressed in the nonepithelial compartment facing the basolateral side of the gastric epithelial cells and in the squamous epithelium of the forestomach. The gastric mRNAs of K13 (5–6-fold, P < 0.05) (GenBank® accession number NM\_010662.1) and the cognate FXR-target

gene Ibabp (30-fold, P < 0.05) were robustly increased by CDCA in WT but not in FXR-KO mice. These data indicated that K13 is also regulated by FXR in murine gastric epithelial cells.

To determine whether K13 (K1C13/UniProtKB/Swiss-Prot number P13646) is co-expressed with FXR in the human stomach, IHC was performed. In normal gastric tissue, K13 staining revealed a net-like pattern within the foveolar epithelium which was absent in GC (Supplementary Figure S1). The  $\sim$ 54 kDa K13 protein was present in whole-tissue lysates of the normal gastric mucosa and in GC biopsies. Total FXR $\alpha$  mRNA levels were determined in a larger series of GC specimens using RT-qPCR primers directed against its common zinc-finger DNA-binding domain. Total FXRα mRNA (GenBank® accession number NM\_0012069) was reduced in 25 out of 30 biopsies (Figure 5D, P < 0.05) of GC patients as compared with matched tumour-free tissue. K13 mRNA (GenBank® accession number NM\_002274) was also decreased in 24 out of 30 GC biopsies (P < 0.05). These results indicate that K13 expression may be dependent on FXR also in vivo.

# FXR deficiency promotes susceptibility to gastric injury in vivo

To examine the role of gastric FXR in vivo, stomach ulcers were induced in C57BL/6 WT (n = 9) and FXR-KO (n = 8) mice by intraperitoneal administration of Indo (35 mg/kg of body weight) for 24 h [18]. The control WT (n = 6) and FXR-KO (n = 6) animals received a mock injection of 0.9 % NaCl. Gastric tissue sections were stained for H&E (haematoxylin and eosin) and injury scores were determined for each mouse stomach (Figure 6A). The control mice did not show any lesions in either genotype. WT mice administered Indo displayed no (score 0, n=2) or superficial (score 1+, n=4) erosive gastritis or had moderate discrete erosive gastritis (score 2+, n=2). In contrast, almost all of the Indo-treated FXR-KO mice exhibited moderate discrete erosive gastritis (score 2 + n = 3) or suffered from severe gastritis with elongated erosions and ulcerations of the gastric mucosa (score 3+, n=3) (Supplementary Table S4 at http://www.BiochemJ.org/bj/438/bj4380315add.htm). The mean injury score and the area of the lesions (mm<sup>2</sup>) were significantly increased in the FXR-KO compared with WT animals (P < 0.05; Figure 6B). The percentage of mice having ulcers was 50% (four out of eight) in FXR-KO and 22% (two out of nine) in WT (Figure 6B). All mice on Indo expressed elevated gastric mRNAs for Tnf $\alpha$ , IL (interleukin)-1 $\beta$  and IL-6 (results not shown) as compared with NaCl-treated mice. Interestingly, only the Indo-treated WT mice showed an increase in gastric Fxr (GenBank® accession number NM\_001163700.1) and K13 (GenBank® accession number NM 010662.1) mRNA (2-fold, P < 0.05) as compared with NaCl-treated littermates. The mRNAs did not change in FXR-KO mice whether treated with Indo or NaCl (Figure 6C). Thus FXR-KO mice showed an enhanced susceptibility to gastric ulceration compared with WT mice. Collectively, these findings in vivo confirmed our in vitro data that gastric FXR prevents apoptosis and cell damage.

# **DISCUSSION**

In the present study, we described a novel role for bile-acid-activated FXR in the protection of human and murine gastric epithelial cells against inflammation-induced damage and identified K13 as a novel FXR-target gene.

FXR mRNA variants have been described in the stomach tissue of humans, rodents and other species [15,16]. FXR $\alpha$ 1/2 and FXR $\alpha$ 3/4 mRNA, as defined by Huber et al. [15], and the  $\sim$ 56 kDa

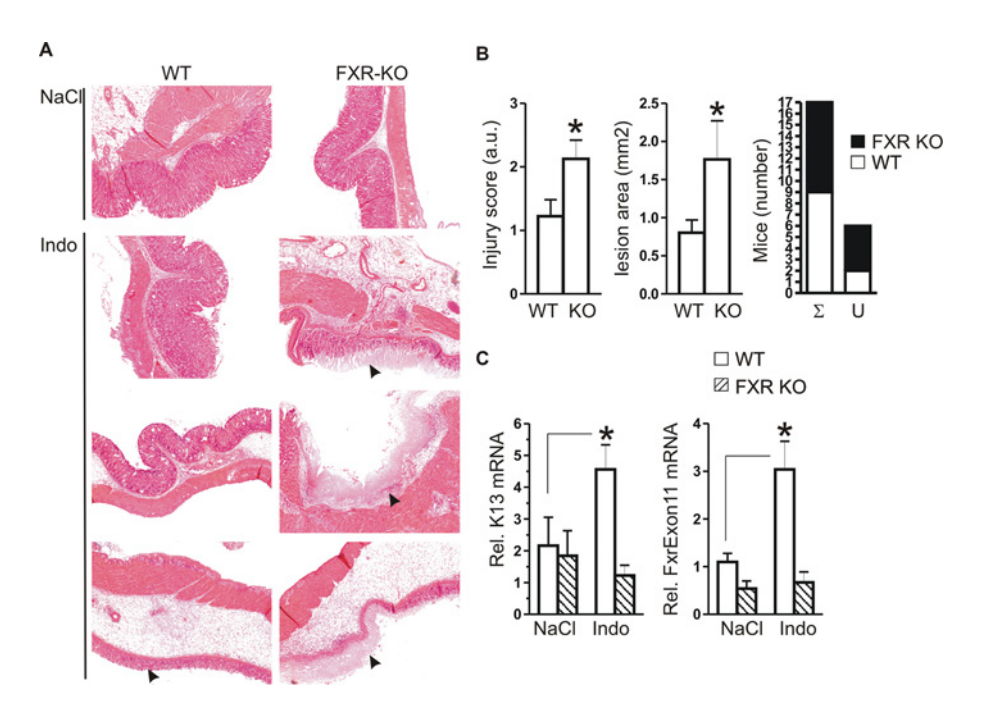


Figure 6 FXR protects against Indo-induced gastric ulceration in vivo

WT and FXR-KO C57BL/6 mice were injected intraperitoneally with Indo (35 mg/kg of body weight) or NaCl ( $n \ge 6$  per group) for 24 h. (**A**) H&E staining with arrows mark the areas of erosion and ulceration. (**B**) Left-hand panel: injury scores in H&E-stained sections of gastric tissues. \*P < 0.05; score 0, no damage; score 1 + , superficial gastritis; score 2 + , moderate discrete gastritis and erosions; score 3 + , severe gastritis with elongated erosions and ulcerations (see also Supplementary Table S4 at http://www.BiochemJ.org/bj/438/bj4380315add.htm). Middle panel: area of lesions in mm². Right-hand panel:  $\Sigma$ , total number of Indo-treated mice; U, number of mice with ulcers per genotype. (**C**) Indo up-regulates K13 (GenBank® accession number NM\_01163700.1) mRNA in stomachs of WT, but not FXR-KO mice. Normalized  $C_T$  values of RT-qPCRs are calculated as the fold change  $\pm$  S.E.M. \*P < 0.05 ( $n \ge 6$  per group).

FXR protein were detected in the non-neoplastic human stomach and in human GC cell lines. In human GC specimens, FXR protein expression was most abundant in I-T GC tissue with IM. IM is considered a potential pre-neoplastic lesion of cancer of the upper-GI tract that is known to be associated with bile acid reflux [2,26,35]. IM is characterized by aberrant transcription factor regulation and altered gene expression [26,36]. Previously, bile acids were shown to up-regulate intestinal differentiation markers (CDX2) and the FXR-target gene SHP in human and rat gastric epithelial cell lines [37,38]. Thus our findings are consistent with the previously described elevation of FXR expression in oesophagitis and in Barrett's IM of the oesophagus [14,25]. Gastrooesophageal reflux disease promotes IM in the gastric cardia [2] and contributes to Barrett's metaplasia and oesophageal carcinogenesis. Duodenogastric reflux that occurs for example as a complication of surgical resection, increases the risk for GC [3]. Thus bile-acid-activated FXR may be part of a protective defence reaction against the chronic irritation and inflammation of the gastric mucosa, which is thought to facilitate the formation of intestinal type GC.

In support of this concept, the present study has shown that ectopic FXR confers resistance to inflammation-induced apoptosis in the human GC cell line AGS, which is naturally devoid of FXR. We identified K13 that, together with other desmosomal components (K6, keratin-associated protein 2-1 and plakophilin 4), is up-regulated in response to FXR and its ligand CDCA, and showed that K13 appears to mediate at least some of the anti-apoptotic effects of FXR. This particular cluster of structural proteins suggests a possible role of FXR in maintaining the epithelial barrier by preserving cell junctions. K13 is a differentiation marker of stratified mucosal epithelia and is also expressed in human GC [39–42].

Consistent with the well-characterized regulation of K13 by retinoids in the squamous epithelium [29–32], we discovered that K13 is up-regulated by CDCA-activated FXR via a conserved RARE *in vitro* and by a CDCA-enriched diet *in vivo*. In addition to their structural functions, keratins such as K8/18 in columnar epithelia directly interfere with apoptotic signalling. Keratins interact with and inhibit the death pathway components TNFR (TNF receptor)/Fas and TRADD (TNF-associated death domain)/FADD (Fas-associated death domain) [27,43–47], suggesting a direct mechanistic link between FXR and K13 to these proteins.

In further support of a protective role of gastric FXR, the present study found that tissue injury evoked by Indo-mediated ulceration [18] of the gastric mucosa was more severe in FXR-deficient mice compared with WT animals. This *in vivo* observation is consistent with previous studies in mouse models of colitis and colon cancer, in which FXR deficiency exacerbated both inflammation [23] and tumorigenesis [10]. In those previous studies, it was suggested that one important mechanism was FXR-mediated transrepression of pro-inflammatory NF- $\kappa$ B (nuclear factor  $\kappa$ B)-regulated genes in myeloid cells [10]. In the present studies, both Fxr and K13 mRNA were up-regulated upon Indo-induced gastric ulceration, suggesting a similar protective role in the non-neoplastic stomach.

In conclusion, the results of the present study suggest that FXR protects against inflammation-induced cell damage in the normal stomach under stress conditions. As a consequence of chronic inflammation, FXR may contribute to the development of I-T GC by promoting resistance to apoptosis in transformed cells. Downregulation of FXR in GC, similar to what has been described in the human colon [10] and Barrett oesophageal [14] cancers, may be a secondary event that leads to a loss of the protective functions exerted by FXR in non-malignant tissue.

# **AUTHOR CONTRIBUTION**

Fan Lian, Xiangbin Xing and Gang Yuan performed the experiments, and collected and analysed the data. Claus Schäfer contributed to the animal work. Sandra Rauser, Axel Walch and Christoph Röcken did the histological staining and the quantitative evaluation. Martin Ebeling worked on the promoter sequence analysis, and Matthew Wright edited and proofread the paper prior to submission. Roland Schmid and Matthias Ebert supervised the project and gave conceptual advice. Elke Burgermeister designed the study, performed the experiments, analysed the data and wrote the paper.

#### **ACKNOWLEDGEMENTS**

We thank Minhu Chen (Department of Gastroenterology, First Affiliated Hospital, Sunyat-Sen University, Guangzhou, China) for support on collaborations and Elke Prade (Department of Chemistry, Technische Universität München, Garching, Germany) for technical help. We thank Hans-Peter Märki (Medicinal Chemistry, F. Hoffmann-Laroche, Basel, Switzerland) for the supply of ligands.

# **FUNDING**

This work was supported by the Deutsche Forschungsgemeinschaft (DFG) [grant number SFB 824], the Deutsche Krebshilfe [grant number 107885], Else Kröner Stiftung [grant number P14/07//A104/06] and the Bundesministerium für Bildung und Forschung (BMBF) [grant number 01EZ0802].

# REFERENCES

- Colleypriest, B. J., Palmer, R. M., Ward, S. G. and Tosh, D. (2009) Cdx genes, inflammation and the pathogenesis of Barrett's metaplasia. Trends Mol. Med. 15, 313–322
- 2 Dixon, M. F., Mapstone, N. P., Neville, P. M., Moayyedi, P. and Axon, A. T. (2002) Bile reflux gastritis and intestinal metaplasia at the cardia. Gut 51, 351–355
- 3 Kondo, K. (2002) Duodenogastric reflux and gastric stump carcinoma. Gastric Cancer **5**, 16–22
- 4 Ovrebo, K. K., Aase, S., Grong, K., Viste, A., Svanes, K. and Sorbye, H. (2002) Ulceration as a possible link between duodenogastric reflux and neoplasms in the stomach of rats. J. Surg. Res. 107, 167–178
- 5 Tanaka, Y., Osugi, H., Morimura, K., Takemura, M., Ueno, M., Kaneko, M., Fukushima, S. and Kinoshita, H. (2004) Effect of duodenogastric reflux on N-methyl-N'-nitro-N-nitrosoguanidine-induced glandular stomach tumorigenesis in *Helicobacter pylori*-infected Mongolian gerbils. Oncol. Rep. **11**, 965–971
- 6 Chen, J. and Raymond, K. (2006) Nuclear receptors, bile-acid detoxification, and cholestasis. Lancet 367, 454–456
- 7 Wang, Y. D., Chen, W. D., Moore, D. D. and Huang, W. (2008) FXR: a metabolic regulator and cell protector. Cell Res. 18, 1087–1095
- 8 Houten, S. M., Watanabe, M. and Auwerx, J. (2006) Endocrine functions of bile acids. EMBO J. 25, 1419–1425
- 9 Gadaleta, R. M., van Erpecum, K. J., Oldenburg, B., Willemsen, E. C., Renooij, W., Murzilli, S., Klomp, L. W., Siersema, P. D., Schipper, M. E. and Danese, S. (2011) Farnesoid X receptor activation inhibits inflammation and preserves the intestinal barrier in inflammatory bowel disease. Gut 60, 463–472
- Modica, S., Murzilli, S., Salvatore, L., Schmidt, D. R. and Moschetta, A. (2008) Nuclear bile acid receptor FXR protects against intestinal tumorigenesis. Cancer Res 68, 9589–9594
- 11 De Gottardi, A., Touri, F., Maurer, C. A., Perez, A., Maurhofer, O., Ventre, G., Bentzen, C. L., Niesor, E. J. and Dufour, J. F. (2004) The bile acid nuclear receptor FXR and the bile acid binding protein IBABP are differently expressed in colon cancer. Dig. Dis. Sci. 49, 982–989
- 12 Swales, K. E., Korbonits, M., Carpenter, R., Walsh, D. T., Warner, T. D. and Bishop-Bailey, D. (2006) The farnesoid X receptor is expressed in breast cancer and regulates apoptosis and aromatase expression. Cancer Res. 66, 10120–10126
- 13 Kaeding, J., Bouchaert, E., Belanger, J., Caron, P., Chouinard, S., Verreault, M., Larouche, O., Pelletier, G., Staels, B., Belanger, A. and Barbier, O. (2008) Activators of the farnesoid X receptor negatively regulate androgen glucuronidation in human prostate cancer LNCAP cells. Biochem. J. 410, 245–253
- 14 De Gottardi, A., Dumonceau, J. M., Bruttin, F., Vonlaufen, A., Morard, I., Spahr, L., Rubbia-Brandt, L., Frossard, J. L., Dinjens, W. N., Rabinovitch, P. S. and Hadengue, A. (2006) Expression of the bile acid receptor FXR in Barrett's esophagus and enhancement of apoptosis by guggulsterone in vitro. Mol. Cancer 5, 48

- 15 Zhang, Y., Kast-Woelbern, H. R. and Edwards, P. A. (2003) Natural structural variants of the nuclear receptor farnesoid X receptor affect transcriptional activation. J. Biol. Chem. 278, 104–110
- Huber, R. M., Murphy, K., Miao, B., Link, J. R., Cunningham, M. R., Rupar, M. J., Gunyuzlu, P. L., Haws, T. F., Kassam, A., Powell, F. et al. (2002) Generation of multiple farnesoid X receptor isoforms through the use of alternative promoters. Gene 290, 35–43
- Burgermeister, E., Xing, X., Rocken, C., Juhasz, M., Chen, J., Hiber, M., Mair, K., Shatz, M., Liscovitch, M., Schmid, R. M. and Ebert, M. P. (2007) Differential expression and function of caveolin-1 in human gastric cancer progression. Cancer Res. 67, 8519–8526
- 17a Lauren, P. (1965) The two histological main types of gastric carcinoma: diffuse and so-called intestinal-type carcinoma. An attempt at a histo-clinical classification. Acta Pathol. Microbiol. Scand. 64, 31–49
- 18 Ebert, M. P., Schafer, C., Chen, J., Hoffmann, J., Gu, P., Kubisch, C., Carl-McGrath, S., Treiber, G., Malfertheiner, P. and Rocken, C. (2005) Protective role of heat shock protein 27 in gastric mucosal injury. J. Pathol. 207, 177–184
- 19 Ebert, M. P., Fei, G., Kahmann, S., Muller, O., Yu, J., Sung, J. J. and Malfertheiner, P. (2002) Increased β-catenin mRNA levels and mutational alterations of the APC and β-catenin gene are present in intestinal-type gastric cancer. Carcinogenesis 23, 87–91
- 20 Xing, X., Burgermeister, E., Geisler, F., Einwächter, H., Fan, L., Hiber, M., Rauser, S., Walch, A., Röcken, C., Ebeling, M. et al. (2009) Hematopoietically expressed homeobox (Hex) is a target of FXR in CDCA induced liver hypertrophy. Hepatology 49, 979–988
- 21 Waseem, A., Alam, Y., Dogan, B., White, K. N., Leigh, I. M. and Waseem, N. H. (1998) Isolation, sequence and expression of the gene encoding human keratin 13. Gene 215, 269—279
- 22 Lefebvre, P., Cariou, B., Lien, F., Kuipers, F. and Staels, B. (2009) Role of bile acids and bile acid receptors in metabolic regulation. Physiol. Rev. 89, 147–191
- 23 Vavassori, P., Mencarelli, A., Renga, B., Distrutti, E. and Fiorucci, S. (2009) The bile acid receptor FXR is a modulator of intestinal innate immunity. J. Immunol. 183, 6251–6261
- 24 Bishop-Bailey, D., Walsh, D. T. and Warner, T. D. (2004) Expression and activation of the farnesoid X receptor in the vasculature. Proc. Natl. Acad. Sci. U.S.A. 101, 3668–3673
- 25 Capello, A., Moons, L. M., Van de Winkel, A., Siersema, P. D., van Dekken, H., Kuipers, E. J. and Kusters, J. G. (2008) Bile acid-stimulated expression of the farnesoid X receptor enhances the immune response in Barrett esophagus. Am. J. Gastroenterol. 103, 1510–1516
- 26 Yuasa, Y. (2003) Control of gut differentiation and intestinal-type gastric carcinogenesis. Nat. Rev. Cancer 3, 592–600
- 27 Gilbert, S., Loranger, A., Daigle, N. and Marceau, N. (2001) Simple epithelium keratins 8 and 18 provide resistance to Fas-mediated apoptosisThe protection occurs through a receptor-targeting modulation. J. Cell. Biol. 154, 763–773
- 28 Varro, A., Hemers, E., Archer, D., Pagliocca, A., Haigh, C., Ahmed, S., Dimaline, R. and Dockray, G. J. (2002) Identification of *plasminogen activator inhibitor-2* as a gastrin-regulated gene: role of Rho GTPase and menin. Gastroenterology **123**, 271–280
- 29 Gilfix, B. M. and Eckert, R. L. (1985) Coordinate control by vitamin A of keratin gene expression in human keratinocytes. J. Biol. Chem. 260, 14026–14029
- 30 Kim, S. Y., Berger, D., Yim, S. O., Sacks, P. G. and Tainsky, M. A. (1996) Coordinate control of growth and cytokeratin 13 expression by retinoic acid. Mol. Carcinog. 16, 6–11
- 31 Steijlen, P. M., Happle, R., van Muijen, G. N. and van de Kerkhof, P. C. (1991) Topical treatment with 13-cis-retinoic acid improves Darier's disease and induces the expression of a unique keratin pattern. Dermatologica 182, 178–183
- 32 Rosenthal, D. S., Griffiths, C. E., Yuspa, S. H., Roop, D. R. and Voorhees, J. J. (1992) Acute or chronic topical retinoic acid treatment of human skin in vivo alters the expression of epidermal transglutaminase, loricrin, involucrin, filaggrin, and keratins 6 and 13 but not keratins 1, 10, and 14. J. Invest. Dermatol. 98, 343–350
- 33 Seol, W., Choi, H. S. and Moore, D. D. (1995) Isolation of proteins that interact specifically with the retinoid X receptor: two novel orphan receptors. Mol. Endocrinol. 9, 72–85
- 34 Winter, H., Fink, P. and Schweizer, J. (1994) Retinoic acid-induced normal and tumor-associated aberrant expression of the murine keratin K13 gene does not involve a promotor sequence with striking homology to a natural retinoic acid responsive element. Carcinogenesis 15, 2653–2656
- Sobala, G. M., O'Connor, H. J., Dewar, E. P., King, R. F., Axon, A. T. and Dixon, M. F. (1993) Bile reflux and intestinal metaplasia in gastric mucosa. J. Clin. Pathol. 46, 235–240
- 36 Csendes, A., Bragheto, I., Burdiles, P., Smok, G., Henriquez, A. and Parada, F. (2006) Regression of intestinal metaplasia to cardiac or fundic mucosa in patients with Barrett's esophagus submitted to vagotomy, partial gastrectomy and duodenal diversion. A prospective study of 78 patients with more than 5 years of follow up. Surgery 139, 46–53
- 37 Park, M. J., Kim, K. H., Kim, H. Y., Kim, K. and Cheong, J. (2008) Bile acid induces expression of COX-2 through the homeodomain transcription factor CDX1 and orphan nuclear receptor SHP in human gastric cancer cells. Carcinogenesis 29, 2385–2393

- 38 Xu, Y., Watanabe, T., Tanigawa, T., Machida, H., Okazaki, H., Yamagami, H., Watanabe, K., Tominaga, K., Fujiwara, Y., Oshitani, N. and Arakawa, T. (2010) Bile acids induce cdx2 expression through the farnesoid x receptor in gastric epithelial cells. J. Clin. Biochem. Nutr. 46, 81–86
- 39 Levy, R., Czernobilsky, B. and Geiger, B. (1992) Cytokeratin polypeptide in gastrointestinal adenocarcinomas displaying squamous differentiation. Hum. Pathol. 23, 695–702
- 40 Taniere, P., Martel-Planche, G., Maurici, D., Lombard-Bohas, C., Scoazec, J. Y., Montesano, R., Berger, F. and Hainaut, P. (2001) Molecular and clinical differences between adenocarcinomas of the esophagus and of the gastric cardia. Am. J. Pathol. 158, 33–40
- 41 Schwerer, M. J. and Baczako, K. (1996) Expression of cytokeratins typical for ductal and squamous differentiation in the human stomach: an immunohistochemical study of normal foveolar epithelium, *Helicobacter pylori* gastritis and intestinal metaplasia. Histopathology 29, 131–137
- 42 Kim, M. A., Lee, H. S., Yang, H. K. and Kim, W. H. (2004) Cytokeratin expression profile in gastric carcinomas. Hum. Pathol. **35**, 576–581

Received 15 December 2010/25 May 2011; accepted 27 May 2011 Published as BJ Immediate Publication 27 May 2011, doi:10.1042/BJ20102096

- 43 Caulin, C., Ware, C. F., Magin, T. M. and Oshima, R. G. (2000) Keratin-dependent, epithelial resistance to tumor necrosis factor-induced apoptosis. J. Cell. Biol. 149, 17–22
- 44 Inada, H., Izawa, I., Nishizawa, M., Fujita, E., Kiyono, T., Takahashi, T., Momoi, T. and Inagaki, M. (2001) Keratin attenuates tumor necrosis factor-induced cytotoxicity through association with TRADD. J. Cell Biol. 155, 415–426
- 45 Ku, N. O., Soetikno, R. M. and Omary, M. B. (2003) Keratin mutation in transgenic mice predisposes to Fas but not TNF-induced apoptosis and massive liver injury. Hepatology 37, 1006–1014
- 46 Gilbert, S., Loranger, A. and Marceau, N. (2004) Keratins modulate c-Flip/extracellular signal-regulated kinase 1 and 2 antiapoptotic signaling in simple epithelial cells. Mol. Cell. Biol. 24, 7072–7081
- 47 Yoneda, K., Furukawa, T., Zheng, Y. J., Momoi, T., Izawa, I., Inagaki, M., Manabe, M. and Inagaki, N. (2004) An autocrine/paracrine loop linking keratin 14 aggregates to tumor necrosis factor β-mediated cytotoxicity in a keratinocyte model of epidermolysis bullosa simplex. J. Biol. Chem. 279, 7296–7303



# SUPPLEMENTARY ONLINE DATA

# Farnesoid X receptor protects human and murine gastric epithelial cells against inflammation-induced damage

Fan LIAN\*, Xiangbin XING\*, Gang YUAN\*, Claus SCHÄFER†, Sandra RAUSER‡, Axel WALCH‡, Christoph RÖCKEN§, Martin EBELING||, Matthew B. WRIGHT||, Roland M. SCHMID¶, Matthias P. A. EBERT\*\* and Elke BURGERMEISTER\*\*

\*Department of Gastroenterology, The First Affiliated Hospital of Sun Yat-sen University, 510275 Guangzhou, China, †Department of Medicine II, Klinikum der Universität München, D-81377 Munich, Germany, ‡Institute of Pathology, Helmholtz Zentrum München, D-85764 Oberschleissheim, Germany, §Institute of Pathology, Christian Albrechts Universität, D-24105 Kiel, Germany, IIF. Hoffmann-La Roche, CH-4070 Basel, Switzerland, ¶Department of Medicine II, Klinikum rechts der Isar, Technische Universität München, D-81675 Munich, Germany, and \*\* Department of Medicine II, Universitätsklinikum Mannheim der Universität Heidelberg, D-68167 Mannheim, Germany

## Table S1 Primers and oligonucleotides

The primers were used for RT–PCR detecting human FXR $\alpha$  mRNA variants (GenBank® accession numbers NM\_005123.2 and NT\_029419.12). The oligonucleotides were used for ChIP and EMSA in the human genomic K13 locus (GenBank® accession number AF049259). E, exon; DBD, DNA-binding domain.

Gene	Amplicon	Sense	Antisense
FXRα1/2	605 bp	5'-AGGGCCTTGAAAGTCCATCT (E1)-3'	5'-AGCTCATCCCCTTTGATCCT (E4)-3'
$\Delta$ FXR $\alpha$ 1/2	350 bp	5'-CATTCCCATTTACCTACCACAGA(E3)-3'	5'-AGCTCATCCCCTTTGATCCT (E4)-3'
$FXR\alpha 3/4$	404 bp	5'-GTAATGCAGTTTCAGGGGTTA(E3a) -3'	5'-AGCTCATCCCCTTTGATCCT (E4)-3'
$FXR\alpha$ total	113 bp	5'-GCATTACCAAAAACGCTGTG(DBD) -3'	5'-TCCCATCTCTTTGCATTTCC(DBD)-3'
K13	-500/+1	5'-GTGACCTTGCAAAGCACAGA-3'	5'-CCTCCATAGGGGCTGGTTAT-3'
K13	RARE1	5'-CGAGGGCTACGGTGACCTTGCAAA-3'	5'-TTTGCAAGGTCACCGTAGCCCTCG-3'
K13	RARE2-WT	5'-GTTCTAATACTGGGTGGGGCTCAG-3'	5'-CTGAGCCCCACCCAGTATTAGAAC-3'
K13	RARE2-MUT	5'-GTTCTAATGTATATTGGAATAAGG-3'	5'-CCTTATTCCAATATACATTAGAAC-3'
K13	RARE3	5'-CTTAAGTGGAGGTGAAACAGAATT-3'	5'-AATTCTGTTTCACCTCCACTTAAG-3'

# Table S2 Bile-acid-regulated human genes in AGS cells identified by DNA microarray

Results are expressed as the fold change of mRNA expression in AGS/FXR compared with AGS/EV cells upon a 16 h stimulation with 100  $\mu$ M CDCA. GO, gene ontology.

Gene name	Symbol	GenBank® accession number	GO-group	Change factor
Up-regulated genes				
Nuclear receptor subfamily 1, group H, member 4 (farnesoid X receptor)	NR1H4 FXR	NM_005123	Transcription	147
Organic solute transporter $\alpha$	OST $\alpha$	NM_152672	Metabolism	48
Keratin 13	KRT13	NM_002274	Epidermal development	42
Serpin peptidase inhibitor, clade B (ovalbumin), member 2	SERPINB2	NM_002575	Antiapoptosis	36
Keratin 6A/keratin 6C/keratin 6E	KRT6A/KRT6C/KRT6E	NM_005554/NM_058242/NM_173086	Ectoderm development	10
Keratin associated protein 2-1	KRTAP2-1	XM_927943	Structural constituent	10
$TNF_{\alpha}$ -induced protein 8	TNFAIP8	NM_014350	Anti-apoptosis	7
Keratin, hair, basic, 1	KRTHB1	NM_002281	Epidermis development	6
Plakophilin 4	PKP4	NM 001005476	Cell adhesion	4
Catenin (cadherin-associated protein), $\alpha$ 1, 102 kDa	CTNNA1	NM 001903	Cell adhesion	3
Down-regulated genes		_		
Progastricsin (pepsinogen C)	PGC	NM 002630	Proteolysis	0.4
Trypsinogen C	TRY6	NR 001296	Proteolysis	0.4
Matrix metallopeptidase 7 (matrilysin, uterine)	MMP7	NM 002423	Peptidoglycan metabolism	0.4
Matrix metallopeptidase 1 (interstitial collagenase)	MMP1	NM 002421	Peptidoglycan metabolism	0.3
Protease, serine, 1 (trypsin 1)	PRSS1	NM_002769	Proteolysis	0.2

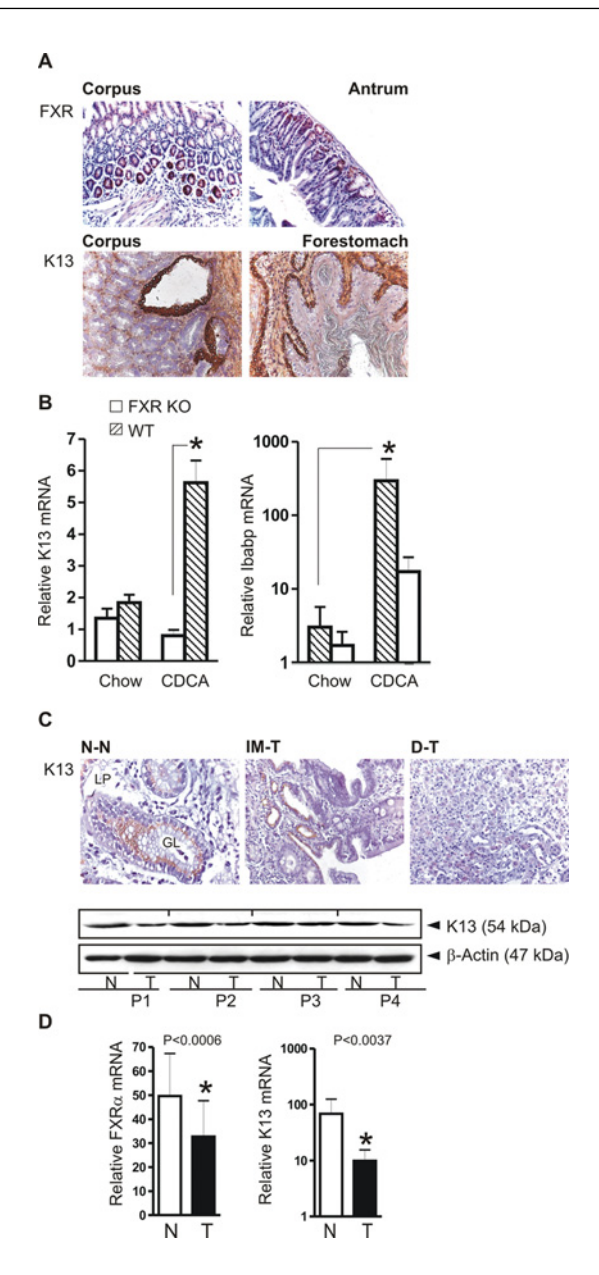


Figure S1 K13 is also regulated by FXR in vivo

(A) Upper panels: detection of FXR (Nr1h4/UniProtKB/Swiss-Prot number Q60641) by IHC in the corpus and antrum regions of stomachs from WT C57BL/6 mice using the rabbit polyclonal antiserum. Lower panels: detection of K13 (K1c13/UniProtKB/Swiss-Prot number P08730) by IHC in the mouse corpus and forestomach regions; magnification 100×. (B) Quantification of K13 mRNA (GenBank® accession number NM\_010662.1) and the cognate FXR-target gene Ibabp in stomachs from WT and FXR-KO mice. Mice were fed on a chow diet with 1 % (w/w) CDCA or a standard mouse chow (control) for 7 days respectively. Normalized C<sub>T</sub> values from RT-qPCRs were calculated as fold changes  $\pm$  S.E.M. (n=5 per group and genotype). \*P <0.05. (C) K13 (K1C13/UniProtKB/Swiss-Prot number P13646) protein is expressed in human GC specimens. Upper panel: detection of K13 by IHC in normal gastric glands (N-N), in I-T GC  $\,$ (I-T) and D-T GC (D-T) tissue. Magnification 200× and 400×. Lower panel: detection of K13 by WB in tissue lysates from tumour and paired non-tumour specimens of four different GC patients. (**D**) Quantification of total FXR $\alpha$  (GenBank<sup>®</sup> accession number NM\_0012069) and K13 (GenBank® accession number NM\_002274.3) mRNA in human GC tissue. Normalized C<sub>T</sub> values from RT–qPCRs are fold change  $\pm$  S.E.M. (n = 30 patients per group) in tumour tissue (T) compared with matched normal (N) tissue;  ${}^*P < 0.05$  (Wilcoxon signed-rank test).

# Table S3 Sequence alignment of a conserved hexameric element (RARE2) in genomic K13 loci

Predicted SP1 sites are marked by italics, functional RARE sites are marked by bold italics and are marked by underlined residues. Rev, reverse; Rev compl., reverse complemented DNA sequence.

M00762	RGG NCA A A/GGG TCA (PPAR, HNF4, COUP, RAR)
Rev compl.	T/CCC AGT
Rev	ACT GGG/A
CK13 Human	ATCTCAGGTCCC-GTTCTAAT <u>ACT GGG</u> TGG <u>GGC TCA</u> G (SP1)
CK13 Mouse	GGTTCAG-TCCCTGTTCTAAT ACT GGG CAG GGC TGGG (RARE)
CK13 Rat	TGTTCAG-TCCCTGTCCTAAT ACT GGG CAG GGC TGGG

# Table S4 Histopathological analysis of gastric ulceration

WT and FXR-KO mice (C57BL/6) were treated for 24 h with Indo (35 mg/kg of body weight, intraperitoneal) or NaCl (0.9 %, intraperitoneal). Injury scores were assigned based on microscopical evaluation of H&E-stained paraffin sections comprising the gastric corpus and antrum regions.

Score	WT	КО	Description
3+	1	3	Severe gastritis, ulcerations and elongated erosions (>5 mm), and fibrinoid vascular necrosis
2+	2	3	Moderate discrete erosive gastritis (<5 mm)
1+	4	2	Superficial discrete erosive gastritis
0	2	0	Normal
Total n	9	8	Number of mice per genotype

Received 15 December 2010/25 May 2011; accepted 27 May 2011 Published as BJ Immediate Publication 27 May 2011, doi:10.1042/BJ20102096